Polycyclic aromatic hydrocarbon contribution to the infrared output energy of the universe at Z 2

Guilaine Lagache, H. Dole, J.-L Puget, G. Perez-gonzalez, E. Le Floc'h, G. H Rieke, C. Papovich, E. Egami, A. Alonso-herrero, C. W Engelbracht, et al.

The Astrophysical Journal Supplement Series, 154:112–117, 2004 September

POLYCYCLIC AROMATIC HYDROCARBON CONTRIBUTION TO THE INFRARED OUTPUT ENERGY OF THE UNIVERSE AT $z \simeq 2$

G. Lagache,[1] H. Dole,[1,2] J.-L. Puget,[1] P. G. Pérez-González,[2] E. Le Floc'h,[2] G. H. Rieke,[2] C. Papovich,[2] E. Egami,[2] A. Alonso-Herrero,[2] C. W. Engelbracht,[2] K. D. Gordon,[2] K. A. Misselt,[2] and J. E. Morrison[2]

Received 2004 March 26; accepted 2004 May 4

ABSTRACT

We present an updated phenomenological galaxy evolution model to fit the *Spitzer* 24, 70, and 160 μm number counts, as well as all the previous mid- and far-infrared observations. Only a minor change of the comoving luminosity density distribution in the previous model (Lagache, Dole, & Puget), combined with a slight modification of the starburst template spectra mainly between 12 and 30 μm, are required to fit all the data available. We show that the peak in the *Spitzer* Multiband Imaging Photometer 24 μm counts is dominated by galaxies with redshift between 1 and 2, with a nonnegligible contribution from the $z \geq 2$ galaxies ($\sim$30% at $S = 0.2$ mJy). The very close agreement between the model and number counts at 15 and 24 μm strikingly implies that (1) the polycyclic aromatic hydrocarbon features remain prominent in the redshift band 0.5–2.5 and (2) the IR energy output has to be dominated by $\sim 3 \times 10^{11}\ L_{\odot}$ to $\sim 3 \times 10^{12}\ L_{\odot}$ galaxies from redshift 0.5 to 2.5. Combining *Spitzer* with *Infrared Space Observatory* deep cosmological surveys gives for the first time an unbiased view of the infrared universe from $z = 0$ to 2.5.

Subject headings: galaxies: evolution — galaxies: high-redshift — infrared: galaxies — ISM: lines and bands

1. INTRODUCTION

A cosmic far-infrared background (CIB) that would trace the peak of the star formation and metal production in galaxy assembly has long been predicted. The first observational evidence for such a background was reported by Puget et al. (1996; see Hauser & Dwek 2001 for a review). This discovery, together with recent cosmological surveys in the infrared (IR) and submillimeter, has opened new perspectives on our understanding of galaxy formation and evolution. The surprisingly large amount of energy in the CIB shows that it is crucial to probe the galaxies contributing to it to understand when and how the bulk of stars formed in the universe.

To understand the sources contributing to the CIB and to interpret the deep source counts, we have developed a phenomenological model that constrains in a simple way the IR luminosity function evolution with redshift and fits all the existing source counts consistent with the redshift distribution, the CIB intensity, and, for the first time, the CIB fluctuation observations from the mid-IR to the submillimeter range (Lagache et al. 2003). *Spitzer* has provided deep new multiwavelength source counts from 24 to 160 μm (Papovich et al. 2004; Dole et al. 2004a). We use these new data to search for a new optimization of the Lagache et al. (2003) model parameters. A remarkable result is that only a minor change of the comoving luminosity density distribution combined with a slight modification of the starburst model spectra, mainly for the 12 μm $\leq \lambda \leq$ 30 μm range, is required to fit all the previous data together with the new constraints.

2. THE MODEL

The model is discussed extensively in Lagache et al. (2003). Our goal is to build the simplest model with the fewest free parameters and separate ingredients. We fix the cosmology to $\Omega_{\Lambda} = 0.7$, $\Omega_0 = 0.3$, and $h = 0.65$. We assume that IR galaxies are mostly powered by star formation, and hence we use spectral energy distributions (SEDs) typical of star-forming galaxies.[3] Although some of the galaxies will have AGN-dominated SEDs, they are a small enough fraction (<10%; Alonso Herrero et al. 2004) that they do not affect the results significantly. We therefore construct "normal" and starburst galaxy template SEDs; a single form of SED is associated with each activity type and luminosity. We assume that the luminosity function (LF) is represented by these two activity types and that they evolve independently. We search for the form of evolution that best reproduces the existing data. The new optimization of the model parameters reproduces (1) the number counts at 15, 24, 60, 70, 90, 160, 170, and 850 μm, (2) the known redshift distributions (mainly at 15 and 170 μm), (3) the local luminosity functions at 60 and 850 μm, and (4) the CIB (from 100 to 1000 μm) and its fluctuations (at 60, 100, and 170 μm).

Compared with the form of the model derived by Lagache et al. (2003), only a slight change of the co-moving luminosity density distribution is required (Fig. 1), together with minor modifications to the starburst template spectra mainly between 12 and 30 μm (Fig. 2). The modified starburst spectra still reproduce the color diagrams of Soifer & Neugeubauer (1991; 12/25 vs. 60/100). We do not modify any other parameters in the model, the SED of the normal galaxy template, the SED of the starburst galaxy templates at longer wavelengths, or the parameterization of the local LF.

Polycyclic aromatic hydrocarbons (PAHs) radiate about 10% of the 1–1000 μm luminosity in a set of features

[1] Institut d'Astrophysique Spatiale, Université Paris-Sud, bât 121, F-91405 Orsay Cedex, France.

[2] Steward Observatory, University of Arizona, 933 North Cherry Avenue, Tucson, AZ 85721.

[3] This assumption is based primarily on observations by ISOCAM and ISOPHOT, but is confirmed by the first *Spitzer* studies of galaxy SEDs in the Lockman Hole and Groth Strip (Le Floc'h et al. 2004; Alonso Herrero et al. 2004).

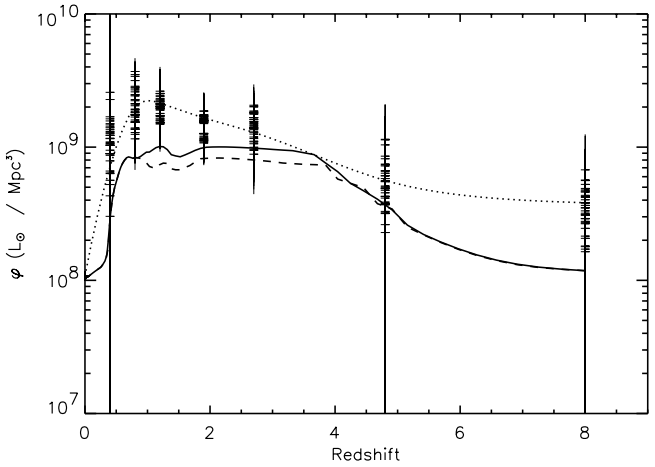

FIG. 1.—Comoving luminosity density distribution of the Lagache et al. (2003) model (*dashed line*) and the updated model presented here (*solid line*). Also shown for comparison is the comoving luminosity density distribution from all cases of Gispert et al. 2000 (*crosses with error bars*), together with the best fit passing through all cases (*dotted line*).

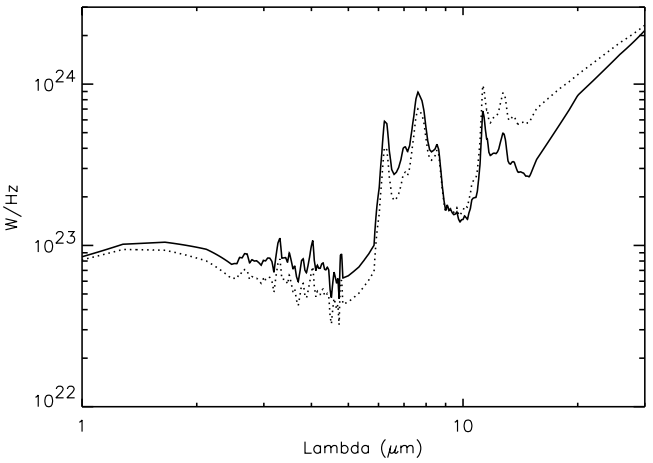

FIG. 2.—Starburst model spectrum for $L = 3 \times 10^{11}\ L_\odot$. *Dashed line*: Lagache et al. (2003); *solid line*: the present updated version of the model. The spectrum has not been modified for $\lambda \geq 30\ \mu$m. The biggest change is about a factor of 2 (for a $3 \times 10^{11}\ L_\odot$ galaxy) around 15 μm.

concentrated mostly between 6 and 15 μm (Fig. 2). This set of features is the strongest spectral concentration known in galaxy spectra. The features strongly affect the mid-IR number counts when the redshift brings them into the bandpass filter. For the 15 μm ISOCAM observations, the peak contribution arises when the 7.7 μm maximum is close to the middle of the band, i.e., $z \sim 0.8$. The ISOCAM 15 μm counts show the existence of a maximum in the redshift distribution just at that redshift. Futhermore, it leads to a maximum in the counts (normalized to the Euclidian, e.g., on Fig. 3), which can exist only when the IR energy output in the critical redshift range is dominated by a well-defined luminosity range. Our model predicts a similar behavior for the 24 μm band.

3. RESULTS

3.1. *Source Counts*

We show the comparison of the number counts at 15, 60, 170, and 850 μm with the observations, as well as the new *Spitzer* 24 μm (Papovich et al. 2004), 70, and 160 μm (Dole et al. 2004a) counts in Figures 3 and 4. The updated model reproduces very well the counts at 15 and 24 μm without any significant changes in the other number counts, as well as the CIB and its fluctuations and the redshift distributions of resolved sources at 15, 60, 170, and 850 μm. The agreement between the observed counts and the model at 24 μm is excellent.

3.2. *First Interpretation of the Spitzer/MIPS Results*

The consistency of the model from the mid-IR and far-IR to the submillimeter indicates that the underlying assumptions are valid up to redshift 2.5. In particular, the very close agreement between the model and number counts at 15 and 24 μm implies that the PAH features remain prominent in the redshift range 0.5–2.5. Furthermore, the well-defined bump in the 24 μm number counts (normalized to the Euclidian) at $S \simeq 0.3$ mJy (Fig. 4) implies at $z \simeq 2$ that $L_{8\,\mu\mathrm{m}} = 3.2 \times 10^{11}\ L_\odot$, which corresponds to $L_{1-1000\,\mu\mathrm{m}} = 3.5 \times 10^{12}\ L_\odot$. These luminosities have to dominate the IR energy output at that redshift (as shown in Fig. 5). As a comparison, an IR energy output dominated by L_* galaxies at $z \simeq 2$ would maximize the 24 μm counts around 3 μJy, which is totally inconsistent with the observation since most of the CIB at 24 μm is resolved at flux densities brighter than $\sim$60 μJy.

Using the new model of IR galaxy evolution, Dole et al. (2004b) have made new determinations of the confusion limits for the Multiband Imaging Photometer for *Spitzer* (MIPS). A summary is provided in Table 1. Figure 6 shows the updated redshift distributions for such confusion-limited surveys. At 24 μm, the deepest surveys will probe star formation up to redshift 3. In the far-IR, MIPS surveys will probe the largely unexplored window $1 \leq z \leq 2$.

In Figure 7, we show the different redshift contributions to the 24 μm number counts. The peak in the counts is dominated by galaxies with redshift between 1 and 2. There is also a nonnegligible contribution from $z > 2$ galaxies (30% at $S = 0.2$ mJy). The integral of the source counts down to 60 μJy gives 1.9 nW m^{-2} sr^{-1}, in excellent agreement with Papovich et al. (2004). It represents about 63% of the CIB at 24 μm. It should also be noted from Figure 7 that the redshift distribution changes sharply for fluxes between 0.3 and 2 mJy. For sources weaker than 150 μJy, the redshift distribution remains about constant.

4. CONCLUSION

We have updated the model of Lagache et al. (2003) to fit the new constraints from *Spitzer* data. We show that only a small change of the co-moving luminosity density distribution and of the starburst template spectra is required to fit all the observations from the mid-IR to the submillimeter. The agreement between the model and all the data demonstrates that the integrated SEDs from galaxies still have prominent 6–9 μm emission from PAH features up to redshift 2.5. It clearly shows that the population of IR galaxies is not dominated by galaxies with featureless continuum spectra (such as AGN-type SEDs in the mid-IR). The fraction of the energy radiated by the PAHs is about one-tenth of the total IR radiation locally and remains roughly constant between redshifts 0.5 and 2.5.

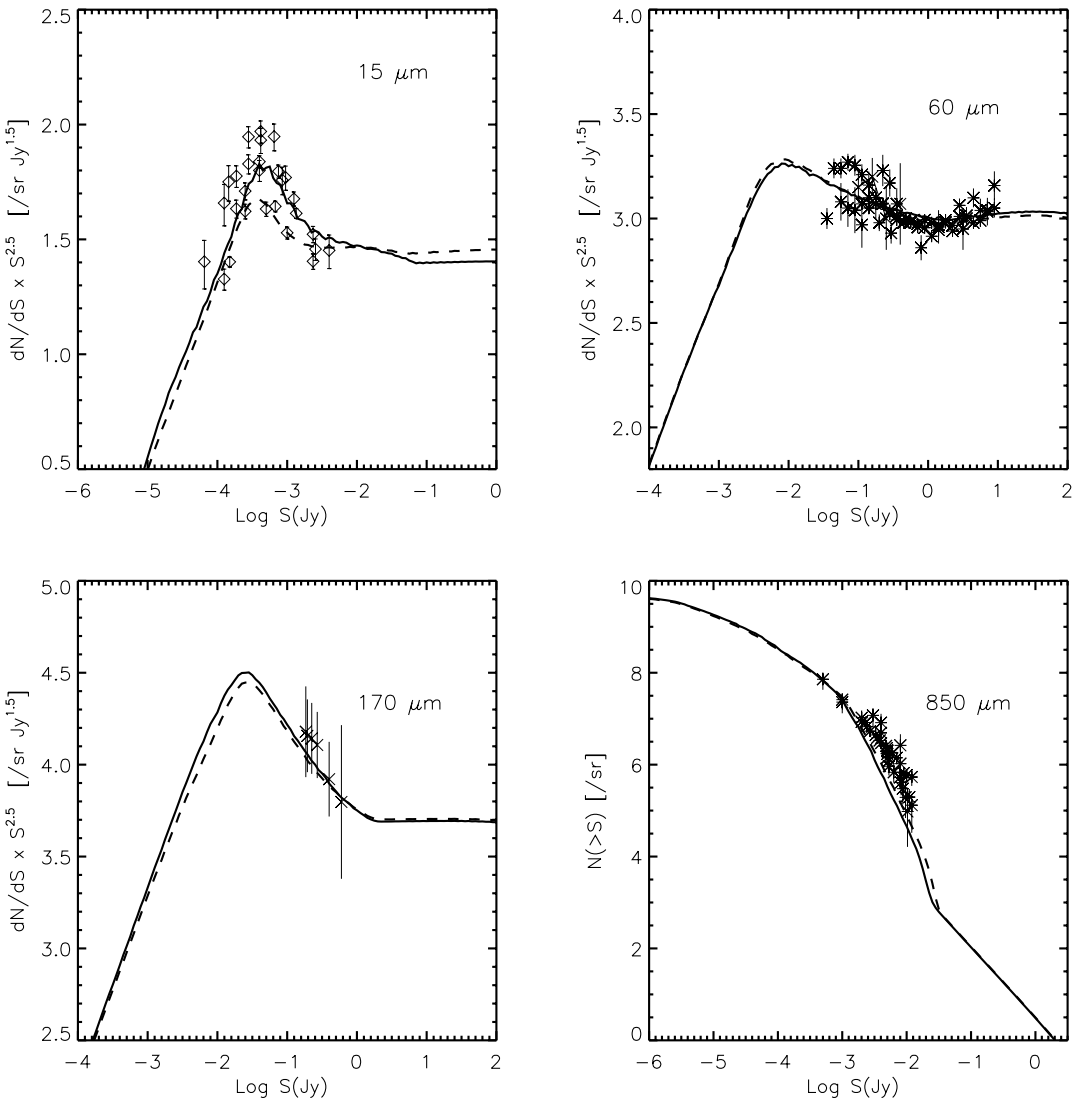

FIG. 3.—Number counts at 15, 60, 170 and 850 μm (in logarithmic scale) together with the model predictions (present work, *solid line*; Lagache et al. 2003, *dashed line*). Data at 15 μm are from Elbaz et al. (1999), at 170 μm from Dole et al. (2001), at 60 μm from Hacking & Houck (1987), Gregorich et al. (1995), Bertin et al. (1997), Lonsdale et al. (1990), Saunders et al. (1990), and Rowan-Robinson et al. (1991), and at 850 μm from Smail et al. (1997), Hughes et al. (1998), Barger et al. (1999), Blain et al. (1999), Borys et al. (2003), Scott et al. (2002), and Webb et al. (2003).

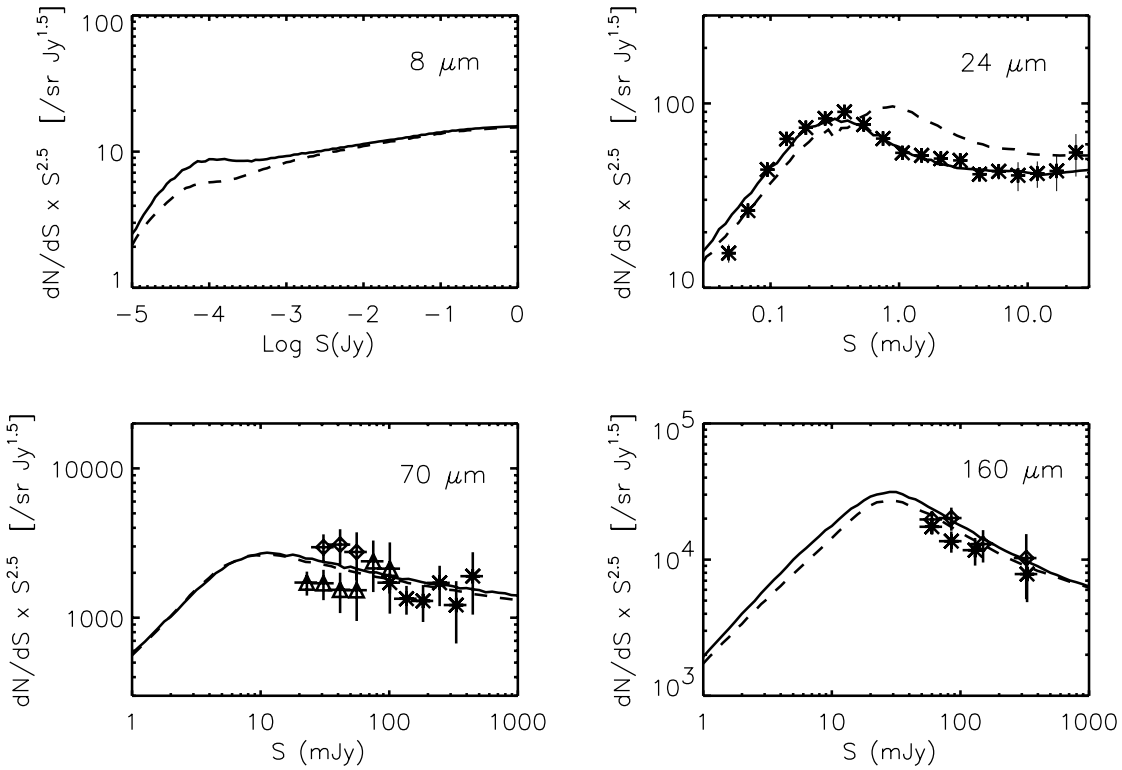

FIG. 4.—Number counts at 24, 70, and 160 μm, together with the model predictions (present work, *solid line*; Lagache et al. 2003, *dashed line*). Data at 24, 70, and 160 μm are from Papovich et al. (2004) and Dole et al. (2004a). Note that none of the observed source counts are corrected for incompleteness.

TABLE 1

1 σ_c CONFUSION NOISE VALUES USING THE BEST CONFUSION ESTIMATOR OF DOLE ET AL. (2003), CONFUSION LIMIT $S_{\rm lim}$, AND THE VALUE OF $q = S_{\rm lim}/\sigma_c$

Parameter	24 μm	70 μm	160 μm
1 σ_c	8.0 μJy	0.47 mJy	10.6 mJy
$S_{\rm lim}$	56 μJy	3.2 mJy	39.8 mJy
q	7.0	6.8	3.8

[a] Using the source density criterion.
[b] In this case, the photometric and source density criteria agree.

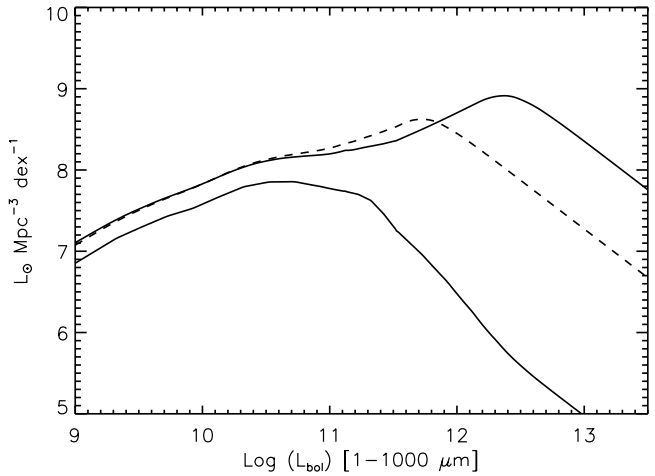

FIG. 5.—Comoving evolution of the IR energy output per dex of luminosity ($L\,dN/d\log L$). The solid, dashed, and triple–dot-dashed lines correspond to $z = 0$, 0.5, and 2, respectively.

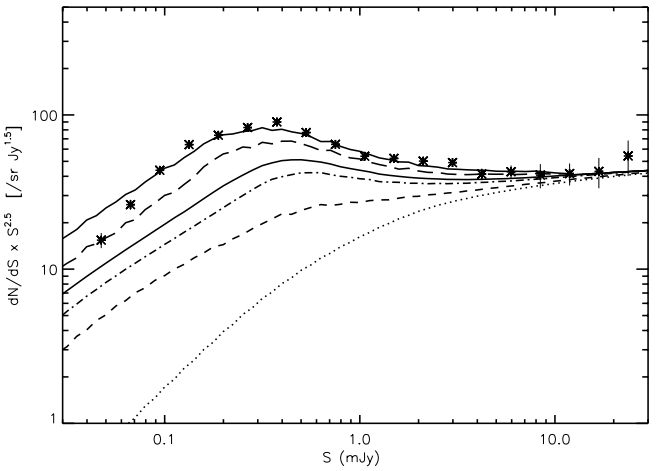

FIG. 7.—Redshift contribution to the number counts at 24 μm. The dotted, dashed, dash-dotted, triple–dot-dashed, and long-dashed lines correspond to the number counts up to redshifts 0.3, 0.8, 1, 1.3, and 2, respectively. Data are from Papovich et al. (2004).

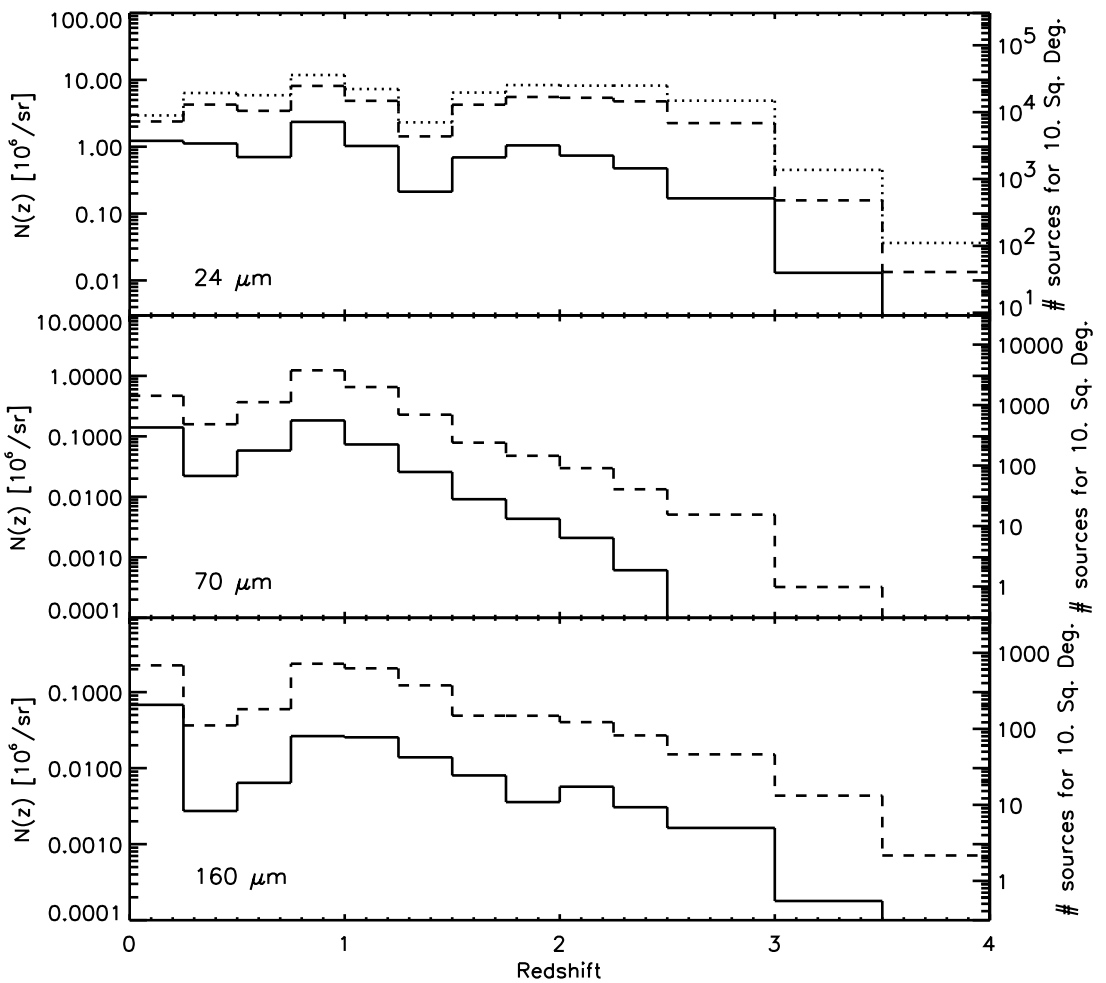

FIG. 6.—MIPS 24, 70, and 160 μm redshift distributions (in logarithmic scale). *Solid lines*: Shallow surveys (flux greater than 0.3, 22.3, and 135.1 mJy at 24, 70, and 160 μm, respectively). *Dashed line*: Deep surveys (flux greater than 0.094, 6.8, and 50.2 mJy at 24, 70, and 160 μm, respectively). *Dotted line*: Ultradeep survey (flux greater than 0.06 mJy at 24 μm).

Our initial model predicted that the IR output energy had to be dominated by galaxies with luminosities increasing rapidly with redshift ($L_{1-1000\ \mu\mathrm{m}} \simeq 3 \times 10^{12}\ L_{\odot}$ at $z = 2.5$; see Fig. 5). This was needed mainly to account for the SCUBA counts (the total energy output at that redshift being mostly driven by the submillimeter extragalactic background level). The excellent agreement between the 24 μm counts and the model confirms strikingly the evolution of the IR luminosity function as being dominated in energy by $\sim 3 \times 10^{11}\ L_{\odot}$ to $\sim 3 \times 10^{12}\ L_{\odot}$ galaxies from redshift 0.5 to 2.5.

We have for the first time with *Spitzer* an unbiased view of the IR universe up to redshift 2.5. With all the mid-IR to submillimeter data, the model is now very well constrained up to $z \simeq 2.5$. Other predictions, together with the number counts of all the planned and future mid-IR to millimeter surveys, will be available on the World Wide Web.[4]

This work is based on observations made with the *Spitzer Space Telescope*, which is operated by the Jet Propulsion Laboratory, California Institute of Technology, under NASA contract 1407. We thank the funding from the MIPS project, which is supported by NASA through the Jet Propulsion Laboratory, subcontract 960785. G. L. warmly thanks the MIPS IT in Tucson, H. D. and J. L. P. for this fruitful collaboration, and G. H. R. for his careful reading of the manuscript.

[4] See http://www.ias.fr/PPERSO/glagache/act/galmodel.html.

REFERENCES

Alonso Herrero, A., et al. 2004, ApJS, 154, 155
Barger, A. J., Cowie, L. L., & Sanders, D. B. 1999, ApJ, 518, L5
Bertin, E., Dennefeld, M., & Moshir, M. 1997, A&A, 323, 685
Blain, A. W., et al. 1999, ApJ, 512, L87
Borys, C., et al. 2003, MNRAS, 344, 385
Dole, H., Lagache, G., & Puget, J.-L. 2003, ApJ, 585, 617
Dole, H., et al. 2001, A&A, 372, 364
———. 2004a, ApJS, 154, 87
———. 2004b, ApJS, 154, 93
Elbaz, D., et al. 1999, A&A, 351, L37
Gispert, R., Lagache, G., & Puget, J.-L. 2000, A&A, 360, 1
Gregorich, D. T., Neugebauer, G., Soifer, B. T., Gunn, J. E., & Herter, T. L. 1995, AJ, 110, 259
Hacking, P. B., & Houck, J. R. 1987, ApJS, 63, 311
Hauser, M. G., & Dwek, E. 2001, ARA&A, 39, 249
Hughes, D. H., et al. 1998, Nature, 394, 241
Lagache, G., Dole, H., & Puget, J.-L. 2003, MNRAS, 338, 555
Le Floc'h, E., et al., 2004, ApJS, 154, 170
Lonsdale, C. J., Hacking, P. B., Conrow, T. B., & Rowan-Robinson, M. 1990, ApJ, 358, L60
Papovich, C., et al. 2004, ApJS, 154, 70
Puget, J.-L., et al. 1996, A&A, 308, L5
Rowan-Robinson, M., Saunders, W., Lawrence, A., & Leech, K. 1991, MNRAS, 253, 485
Saunders, W., et al. 1990, MNRAS, 242, 318
Scott, S. E., et al. 2002, MNRAS, 331, 817
Smail, I., Ivison, R. J., & Blain, A. W. 1997, ApJ, 490, L5
Soifer, B. T., & Neugebauer, G. 1991, AJ, 101, 354
Webb, T. M. A., et al. 2003, ApJ, 587, 41